DESIGN STATUS OF THE PEFP RCS*

J. H. Jang#, H. J. Kwon, H. S. Kim, Y. S. Cho, PEFP/KAERI, Daejeon, Korea
Y. Y. Lee, BNL, Upton, New York 11973, U.S.A.

Abstract

The 100-MeV proton linac of the proton engineering frontier project (PEFP) can be used as an injector of a rapid cycling synchrotron (RCS). The design study of the RCS is in process. The main purpose of the RCS is a spallation neutron source. The initial beam power is 60 kW where the injection and extraction energies are 100 MeV and 1 GeV, respectively. It will be extended to 500 kW through the upgrades of the injection energy to 200 MeV, the extraction energy to 2-GeV, and the repetition rate from 15 Hz to 30 Hz. The slow extraction option is also included in the design for basic and applied science researches. This work summarized the present design status of the PEFP RCS. In the introduction, the present status of the PEFP project is briefly summarized.

INTRODUCTION

Proton Engineering Frontier Project (PEFP) is the 100-MeV proton linac development project which was launched at 2002 and will be finished at 2012 [1]. As an extension plan of the linac, we are considering a rapid cycling synchrotron (RCS). The main purpose of the RCS is a spallation neutron source which can be used in the fields of the material science, bio technology, chemistry, etc.

The PEFP proton linear accelerator consists of two parts. The low energy part includes an ion source, a low energy beam transport (LEBT), a 3-MeV radio frequency quadrupole (RFQ), and a 20-MeV drift tube linac (DTL) [1]. The high energy part consists of seven DTL tanks which accelerator proton beams from 20 MeV to 100 MeV. The 20-MeV linac system has been successfully installed and tested at the KAERI site. The fabrication of the remaining DTL tanks will be finished in this year and the test of the DTL tanks is in progress. A medium energy beam transport (MEBT) system will be installed after the 20-MeV DTL. It includes a 45-degree bending magnet in order to extract 20-MeV proton beams. 100-MeV proton beams will be guided into beam lines by another 45-degree dipole magnet which is located after the last DTL tank. The 20-MeV or 100-MeV proton beams are distributed respectively into 5 target rooms. The main characteristics of PEFP beam lines is using AC magnets to distribute proton beams into 3 target rooms in both 20-MeV and 100-MeV beam lines. The schematic plot of the PEFP linac and beam lines is given in Figure 1. The basic parameters of the linac are summarized in Table 1.

*This work was supported by Ministry of Education, Science and Technology of the Korean government
#jangjh@kaeri.re.kr

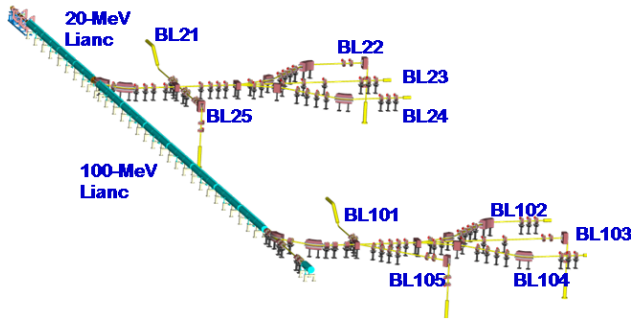

Figure 1: Schematic plot of the PEFP linac and beam lines.

Table 1: Basic Parameters of PEFP Linac

Parameter	Value
Particle	Proton
Beam Energy	100 MeV
Operation Mode	Pulsed
Max. Peak Current	20 mA
Pulse Width	<1.33 ms (< 2.0 ms up to 20 MeV)
Max. Beam Duty	8% (24% up to 20 MeV)

Gyeongju city which is located in the south-eastern part of Korea hosted the project in January 2006. The geological surveys of the site and the site-dependent plan such as the facility layout and access road have been completed for the civil construction. The general arrangement of the accelerator and beam utilization buildings and conventional buildings are also completed. Figure 2 shows the bird's eye view of the PEFP accelerator research center. Now the construction of each building is in progress.

Figure 2: PEFP accelerator research center.

For future extension plans of PEFP, we are studying two options: a superconducting linac (SCL) and a rapid cycling synchrotron (RCS). The main purpose of the extension is a spallation neutron source. An SCL should be an optimal solution for extending the linac energy. We are now studying an elliptical cavity with the design beta of 0.42 [2]. It can be used to accelerate proton beams from 100 MeV to 200 MeV. The cavities with β_g=0.61 and 0.81 will be used for 1-GeV linac. The prototype of the Nb cavity has been successfully fabricated and tested as shown in Figure 3 [3]. The 100-MeV proton linac can be an injector of an RCS whose extraction energy is 1-2 GeV [4]. The main purpose is a spallation neutron source with a fast extraction system. The RCS includes a slow extraction option which is used for radioisotope production, medical application, and basic science. The RCS design is the main part of this paper.

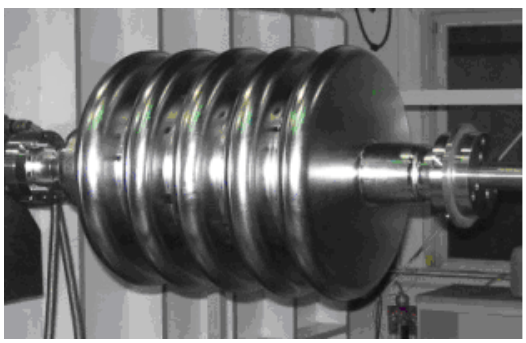

Figure 3: PEFP low beta superconducting cavity.

PEFP RCS DESIGN

As described in a physics design of the RCS [4,5,6], the basic design concepts of the PEFP RCS are as follows,

- The 100-MeV linac is the injector of the RCS.
- At the initial stage, the extraction energy is 1GeV and the beam power is 60 kW.
- The RCS should be upgradable in an injection energy, an extraction energy, and a repetition rate.
- The beam extraction methods includes both a fast extraction for the spallation neutron source and a slow extraction for the other purposes including medical research and RI production.
- The uncontrolled beam loss should be less than 1 W/m for hands-on maintenance.

The upgrade path of the RCS is summarized in Table 2 The beam power of the RCS is 60 kW in the initial stage and finally becomes 500 kW through the three-step upgrade. In the final stage, the injection energy is 200-MeV and the extraction energy is 2 GeV. This work summarized the lattice design and the beam dynamics study on the PEFP RCS. Table 3 summarizes the basic parameters of the RCS for this design study.

Table 2: Upgrade Plan of PEFP RCS

Stage	Injection Energy	Extraction Energy	Repetition Rate	Beam Power
Initial	100 MeV	1 GeV	15 Hz	60 kW
1	100 MeV	1 GeV	30 Hz	120 kW
2	100 MeV	2 GeV	30 Hz	250 kW
3	200 MeV	2 GeV	30 Hz	500 kW

Table 3: Design Parameters PEFP RCS in the Initial Stage

Injected Particle	H-
Lattice Structure	FODO
Super-period	4
Number of Cell	20
Number of Dipoles	32
Machine Tune [Qx /Qy]	4.39 / 4.29
Transition γ	4.4
Circumference [m]	224.16
RF Harmonic	2
RF Voltage	75 kV

The PEFP RCS has a four-fold symmetry in order to reduce the lower order resonance. The basic lattice is a regular FODO structure and one super-period includes five FODO cells. The lattice structure of the RCS was given in Figure 4. The four dispersion-free straight sections are reserved for injection and extraction, RF cavities and beam collimation. The arc straight sections can be used for the momentum collimation and slow extraction. The lattice functions are given in Figure 5 [4].

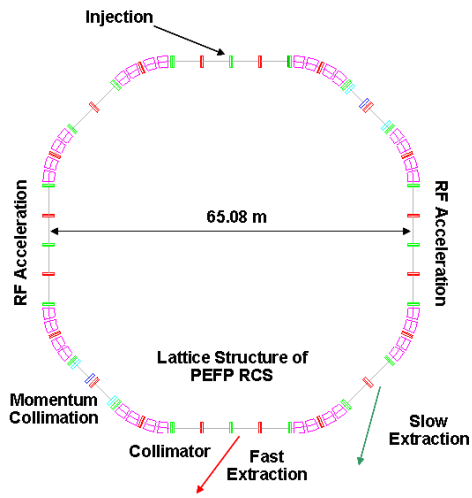

Figure 4: PEFP RCS lattice.

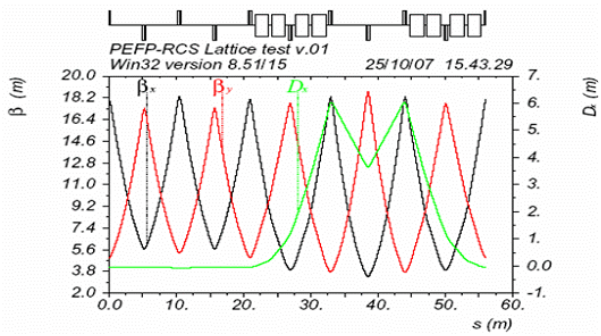

Figure 5: Beta functions and dispersion function in a super-period of the PEFP RCS.

The RF harmonic is two in this RCS and there are two bunches in a synchrotron pulse [6,7]. The linac beam has to be chopped in order to reduce beam losses in the capture and acceleration process. In the 15-Hz operation, one macro-pulse of linac beams includes 400 mid-pulses with the pulse width of 500 ns. It corresponds to the chopping factor of 57%. In the RCS, there are two bunches in a pulse. After a injection period, 200 linac pulses are injected into each RF bucket. The proton number in a synchrotron pulse is 2.5×10^{13}. The time structure of the linac and RCS beams is given in Figure 6.

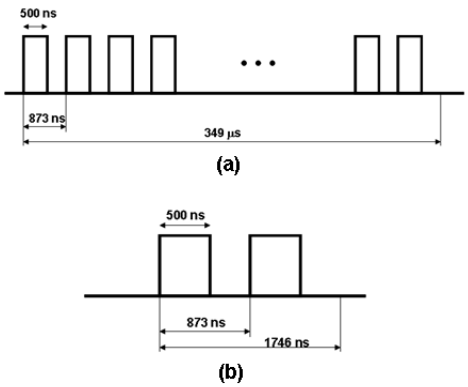

Figure 6: Time structure of (a) mid-pulses in a macro-pulse of linac beams and (b) bunches in a pulse of the RCS beams.

The injection of the PEFP RCS is based on H^- charge exchange injection with a transverse painting method [6, 8]. The injection system consists of a chicane magnet which deforms the horizontal DC orbit up to 105 mm and the four ferrite cored magnets which are used for the fast change of the painting bump in the horizontal and vertical directions. The overall scheme of RCS injection is illustrated in Figure 7 [5]. The particle distributions in x-y, x-x' and y-y' spaces after finishing injection with a correlated painting are given in Figure 8. In this simulation we used ORBIT code [9] with 40,000 macro particles [5]. The particle distributions in x- and y-axis are given in Figure 9 which shows the parabolic distribution as expected in a uniform painting in the transverse phase space [5]. The emittance variations are given in Figure 10 as a function of injection turns in the horizontal and vertical directions [5]. The figures include 90%, 95%, 99%, and 99.9% emittance values. The 99.9% emittance becomes about 300 π mm-mrad.

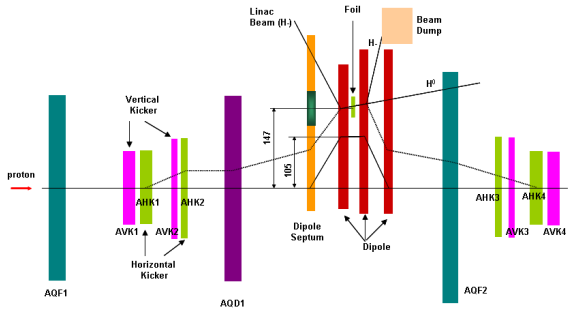

Figure 7: Layout of the injection system for PEFP RCS.

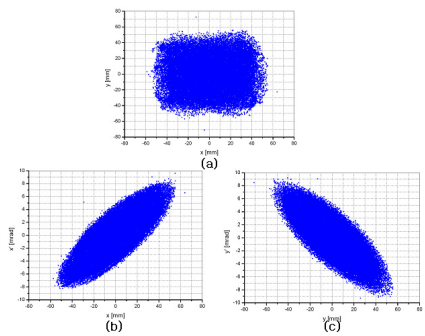

Figure 8: Particle distribution after injection with correlated painting in (a)x-y space, (b) x-x' space, and (c) y-y' space.

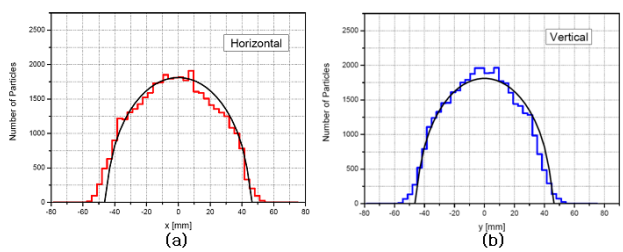

Figure 9: Particle distribution in (a) horizontal and (b) vertical directions.

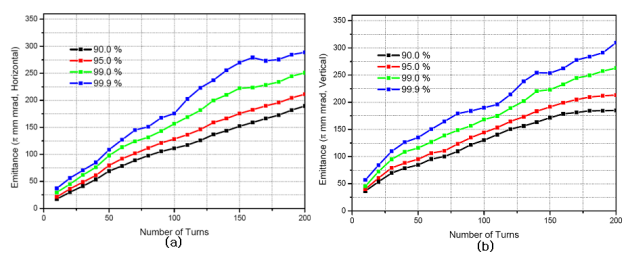

Figure 10: Emittances as a function of injection turns in (a) horizontal and (b) vertical directions.

In order to cure the distorted orbit which is generated by the manufacturing and installation errors of the magnets, we considered 40 corrector magnets which are located just after the quadrupole magnets. The 40 beam position monitors (BPM) are installed near the entrance region of the quadrupole magnets. We assumed that the deviation of field strength less than 0.1% and the displacement and rotation errors are less than 300 m and 1 mrad, respectively. Figure 11 shows the closed orbit distortion and the corrected orbit in the horizontal and vertical direction.

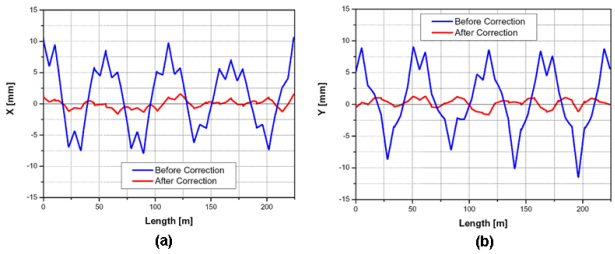

Figure 11: Closed orbit distortion before and after correction (a) in the horizontal direction and (b) in the vertical direction.

The natural chromaticity of the PEFP RCS is $\Delta Q_x/(\Delta p/p)$= -4.3 and $\Delta Q_y/(\Delta p/p)$= -4.6. Assuming a momentum spread of ±1.0%, the tune spread due to the natural chromaticity become ±0.043 in the horizontal plane and ±0.046 in the vertical plane. We note that the tune shift by the chromaticity is very small. In order to correct the chromaticity we studied three schemes of the sextupole combinations: 2-family, 4-family, 6-family scheme as shown in Figure 12. In order to obtain the sextupole strength, we used the HARMON routines in MAD8 programs [10]. Figure 13 shows the tune shifts in with and without chromaticity corrections in the horizontal and vertical directions.

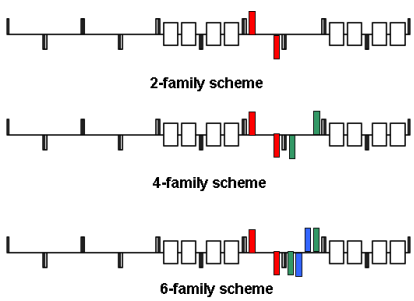

Figure 12: Schematic plot of (a) 2-family, (b) 4-family, and (c) 6-family schemes for the chromaticity corrections.

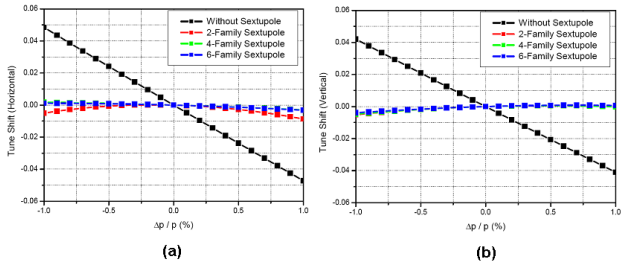

Figure 13: Schematic plot of (a) 2-family, (b) 4-family, and (c) 6-family schemes for the chromaticity corrections.

We also studied the dynamic aperture of the PEFP RCS in the initial operation [11]. The main focuses are the effects of the fractional momentum spread, magnet misalignment, magnet amplitude errors and magnet multi-pole components of dipole magnets. For the simulation, we used the DYNAP routine in MAD8 [10]. Because the maximum value of the fractional momentum deviation is 0.7 % in the injection and acceleration simulation [11], we studied its effects on the dynamic aperture by varying from 0.0% to ±0.7%. Figure 14 shows the dynamics aperture depending on the fractional momentum deviation. The blue curve describes the stable beam region which is given by $\sqrt{\frac{2\beta\varepsilon}{\pi}}+\eta\frac{\delta p}{p}+cod$ where β and ε represent the beta function and beam emittance. The parameter η is the dispersion function of the ring. The cod represents the closed orbit distortion which is less than 1 mm after the orbit correction. This closed orbit distortion effects on the dynamic aperture is given in Figure 15. We assumed that the displacement and rotation errors of the magnets are less than 300 μm and 1 mrad, respectively, and the magnet field errors are less than 10^{-4}. Each quadrupole magnet has a corrector magnet. We found the dynamic aperture moves to outside (red line) of the stable region after the orbit correction even though it is inside (black line) before correction. Finally we studied the dynamic aperture variation by the multi-pole components of the bending magnet. The errors include quadrupole, sextupole, and octupoles which are assumed to be less than 10^{-4} of the dipole amplitude. We found that the effects can be negligible.

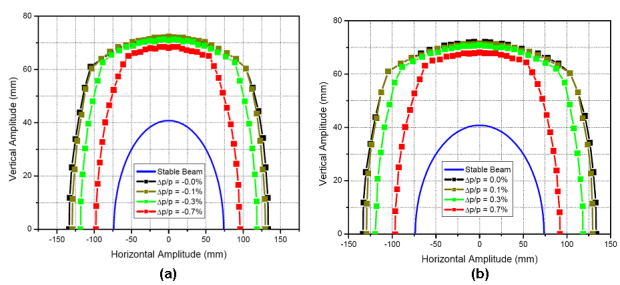

Figure 14: Fractional momentum deviation and dynamic aperture in the LIE algebra tracking method: (a) 0 ~ -0.7 %, (b) 0 ~ 0.7%.

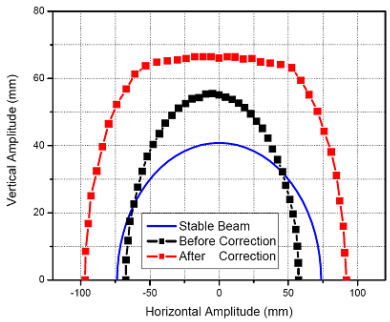

Figure 15: Orbit distortion and dynamic aperture: black line before correction and red line after correction.

Next we performed the acceleration simulation in order to study the magnet and RF ramping for the large capture rate [6,7]. In this study we used a sinusoidal ramping of the magnetic field (Figure 16 (a)). The RF voltage program and the corresponding synchronous phase variation are given in Figure 8(b) and 8(c), respectively. The initial RF voltage is 18.7 kV and the maximum voltage is 75.0 kV. The synchronous phase increases up to about 35 degrees. We used the RAMA program to get the initial ramping of the RF voltage [12]. Figure 17(a) shows the particle distribution in the longitudinal phase space just after injection. We found that there is no beam loss up to 200 injection turns. The particle distribution is given in Figure 17(b) for 1GeV beams. The final energy and capture rate are 1.003 GeV and 99.91%, respectively. The most beam loss happens in the initial ramping stage [6,7].

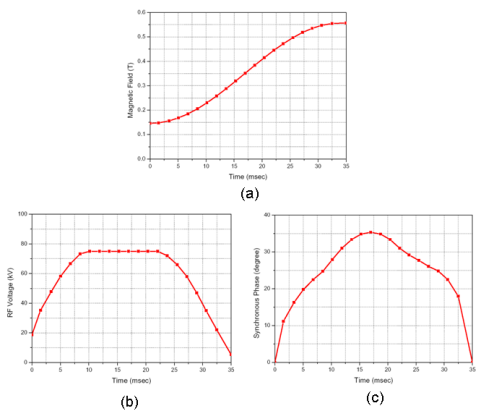

Figure 16: Ramping of (a) magnetic field, (b) RF voltage and (c) the synchronous phase.

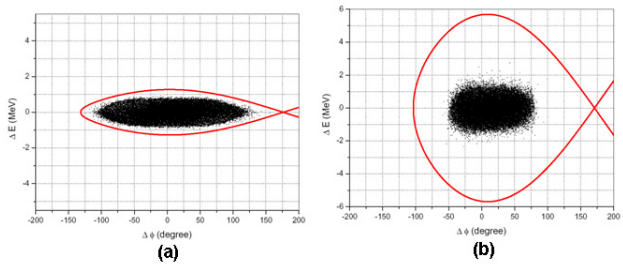

Figure 17: Particle distribution in the RF bucket: (a) just after injection and (b) after full acceleration for 1 GeV.

CONCLUSION

This work summarized the results on the lattice design and the beam dynamics study of the PEFP RCS in the initial stage where the beam power is 60 kW with a 15–Hz operation. The injection and extraction energies are 100 MeV and 1 GeV, respectively.

REFERENCES

[1] J. Jang, Y. Cho, B. Choi, J. Kim, K. Kim, J. Park, "The Korean Proton Engineering Frontier Project", HB 2008, Nashville, August 2008.
[2] A. Sun, L. Zhang, Y. Tnag, Y. Li, C. Gao, Y. Cho, B. Choi, "Status of the PEFP Superconducting RF project", EPAC'08, Genoa, 2008.
[3] H. Kim, H. Kwon, Y. Cho., "Prototyping Activities of Low-beta SRF Cavity for the PEFP Proton Linac Extension", Linac'10, Tsukuba, September 2010.
[4] B. Chung, Y. S. Cho, Y. Y. Lee, "Conceptual Design of the PEFP Rapid Cycling Synchrotron", PAC'07, Albuquerque, June 2007.
[5] J. H. Jang, H. J. Kwon, Y. S. Cho, Y. Y. Lee, "Physics Design of the PEFP RCS", PAC'09, Vancouver, Canada, May 2009.
[6] J. H. Jang, H. J. Kwon, H. S. Kim, Y. S. Cho, Y. Y. Lee, "Design of the PEFP RCS", IPAC 2010, Kyoto, May 2010.
[7] J. H. Jang, H. J. Kwon, Y. S. Cho, Y. Y. Lee, "Acceleration Simulation of PEFP RCS for a 1-GeV Extraction", Korean Nuclear Society Spring Meeting, 2009.
[8] J. H. Jang, Y. S. Cho, Y. Y. Lee, "Injection Simulation Result of th PEFP RCS", Korean Physical Society Autumn Meeting, 2008.
[9] J. Galambos, J. Holmes, D. Olsen, A. Luccio, J. Beebee-Wang, "ORBIT User Manual", 1999.
[10] H. Grote and F. C. Iselin, "The MAD Program: Users Reference Manual", Version 8.19, CERN/SL/90-13.
[11] J. H. Jang, Y. S. Cho, H. J. Kwon, H. S. Kim, "Dynamic Aperture of PEFP RCS", Korean Nuclear Society Autumn Meeting, 2009.
[12] R. Baartman, H. Schonauer, "RAMA: A Computer Code Useful for Designing Synchrotrons", TRI-DN-86-15,1986.